A critical re-assessment of the primary productivity of the Yellow Sea, East China Sea and Japan Sea/East Sea LMEs

Sinjae Yoo[1], Christina Eunjin Kong[1],
Young Baek Son, and Joji Ishizaka[2]

[1]KIOST, Jeju, South Korea
[2]Nagoya Univ, Japan

8th CJK IMBeR Symposium
Sep 18, 2018

Deep Sea Research II, in press

Importance of the primary productivity in the Large Marine Ecosystems (LMEs)

LMEs

- Occupy less than 10% of the world ocean by surface area but support over 80% of the world fish yield (Sherman and Alexander, 1986; Pauly and Lam, 2016).
- An important component in the Earth's biogeochemical system (Liu et al., 2010).

Relationship between primary production and fisheries yield (I)

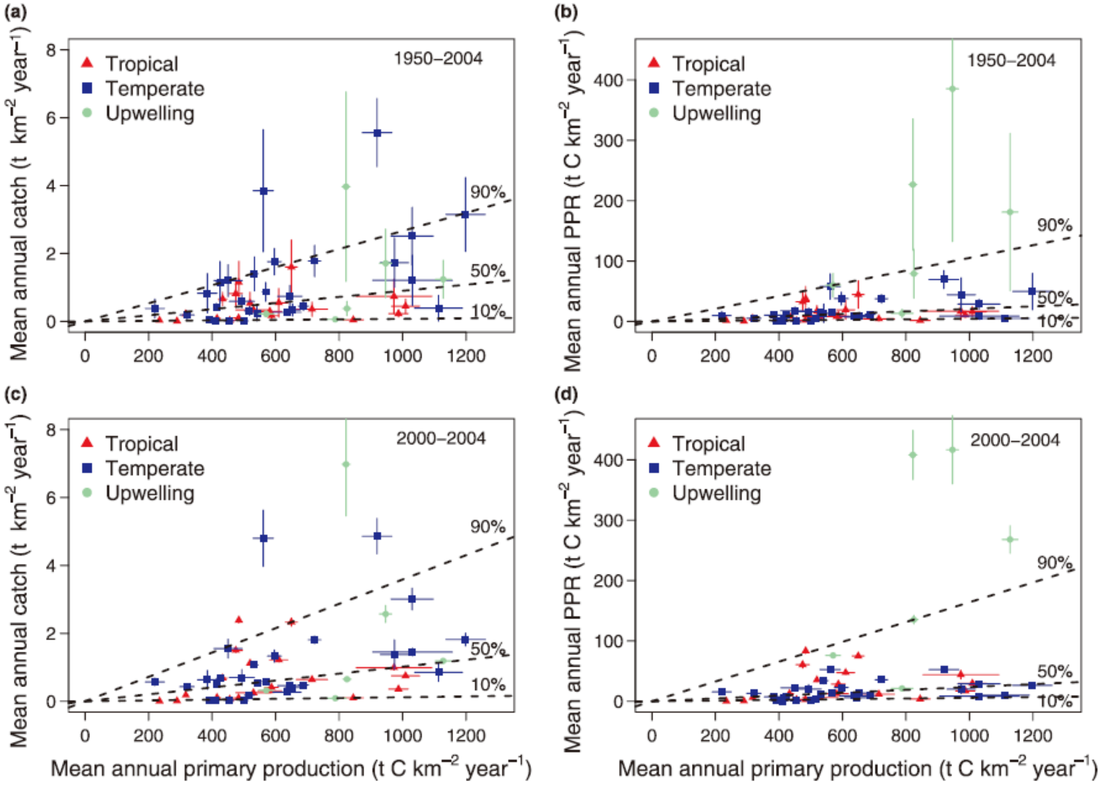

Figure 1 Global marine primary production (PP) and fisheries production expressed in (a,c) catch (t km^{-2} year^{-1}) and (b,d) primary production required (PPR) to sustain catches (in t C km^{-2} year^{-1}) over the long-term period (1950–2004) and recent period (2000–2004). Solid lines indicate quantile regressions models with quantile = 10%, 50%, and 90%.

Chassot et al., 2010

PP determines the upper limit of the global fisheries yields.

Are the seas in the northwestern Pacific more productive than other seas in NP, or are they?

East China Sea

Yellow Sea

East Sea

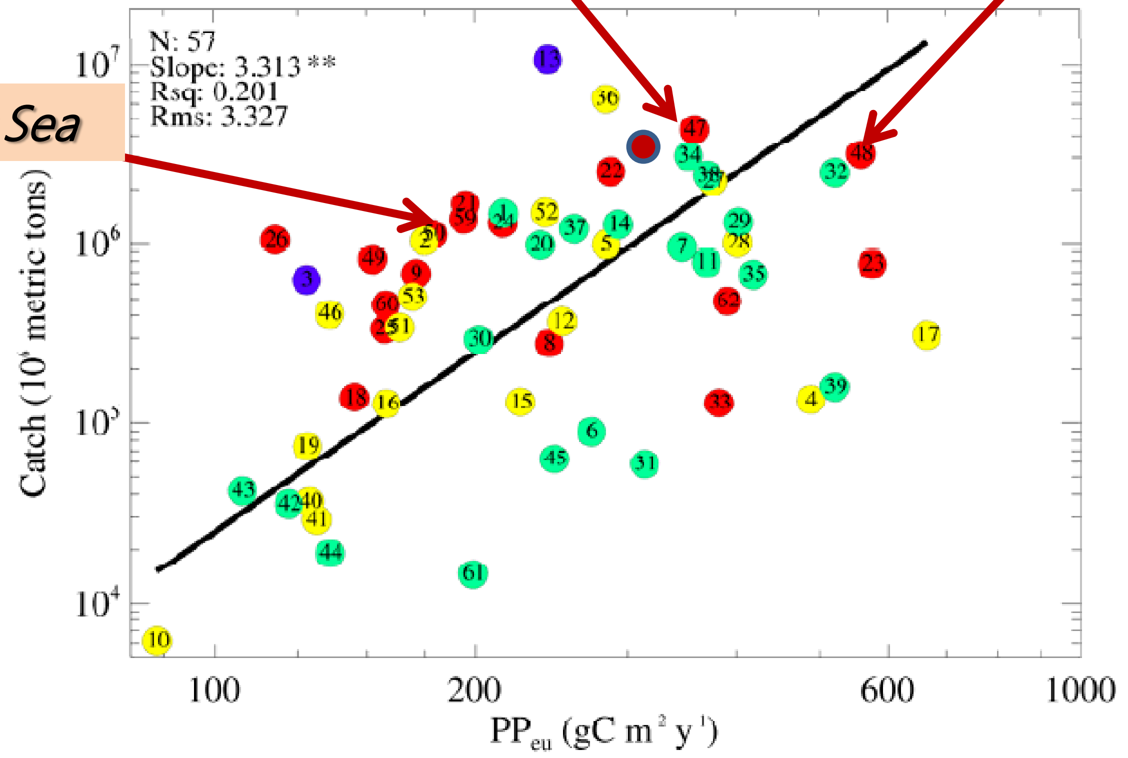

Figure 5A. Positive correlation of 5-yr. mean annual fisheries biomass yield with 9-yr. mean annual primary production in fast warming (red), moderately warming (yellow) and slower warming (green) LMEs. The two blue circles represent cooling LMEs. P<0.001.

UNEP LME Report,
Sherman and Hempel (2009)

Motivation of this study

- The PP of many coastal LMEs tends to be overestimated by erroneous estimates of core variables.
- What are the best algorithms for the three core variables of PP in the three LMEs?
- How do the new PP estimates using these parametrizations compare with the estimates from the global assessments of the UNEP/LME Report and the SAU Project?

SeaWiFS CHL in June 2000

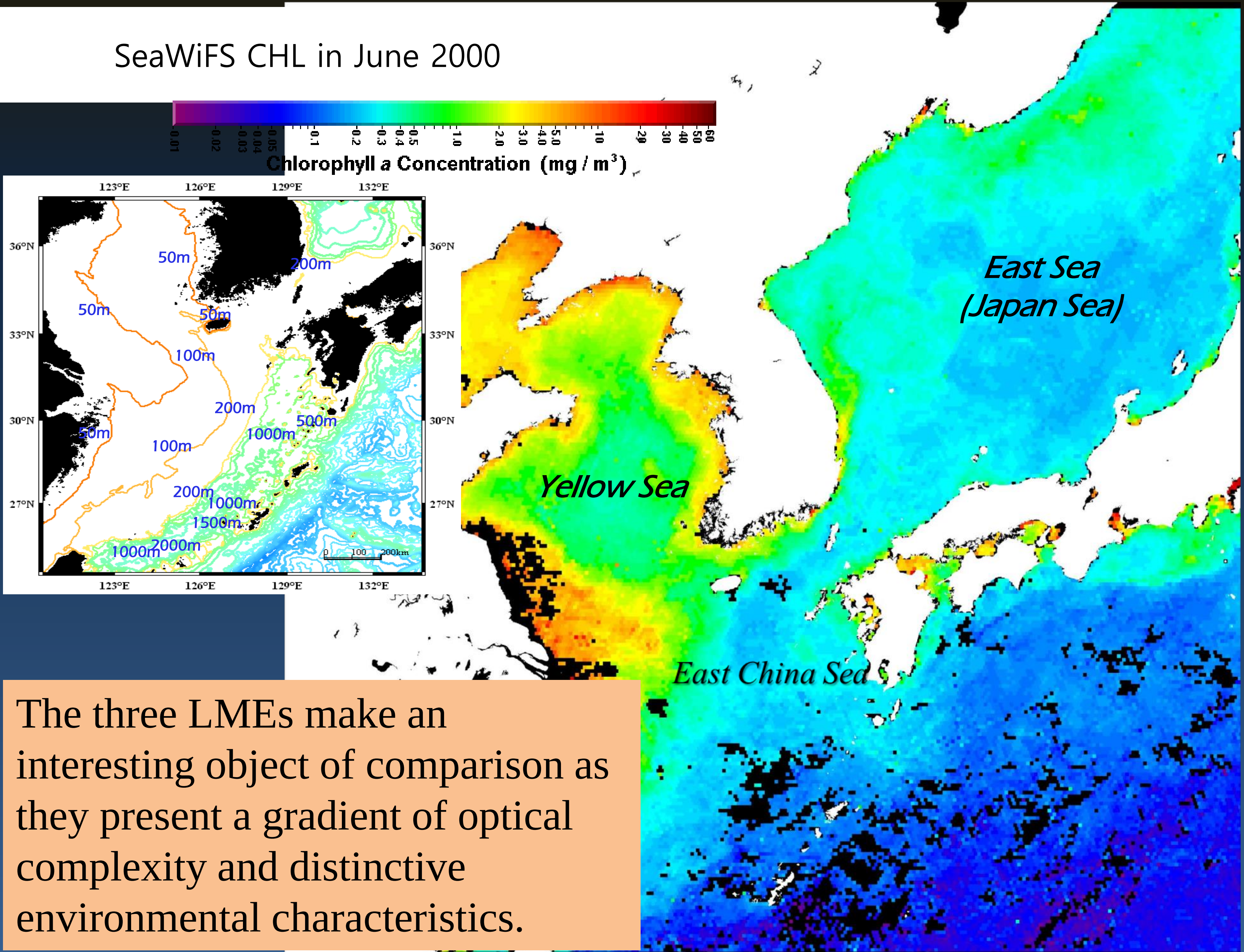

The three LMEs make an interesting object of comparison as they present a gradient of optical complexity and distinctive environmental characteristics.

Daily and hourly in wa colu

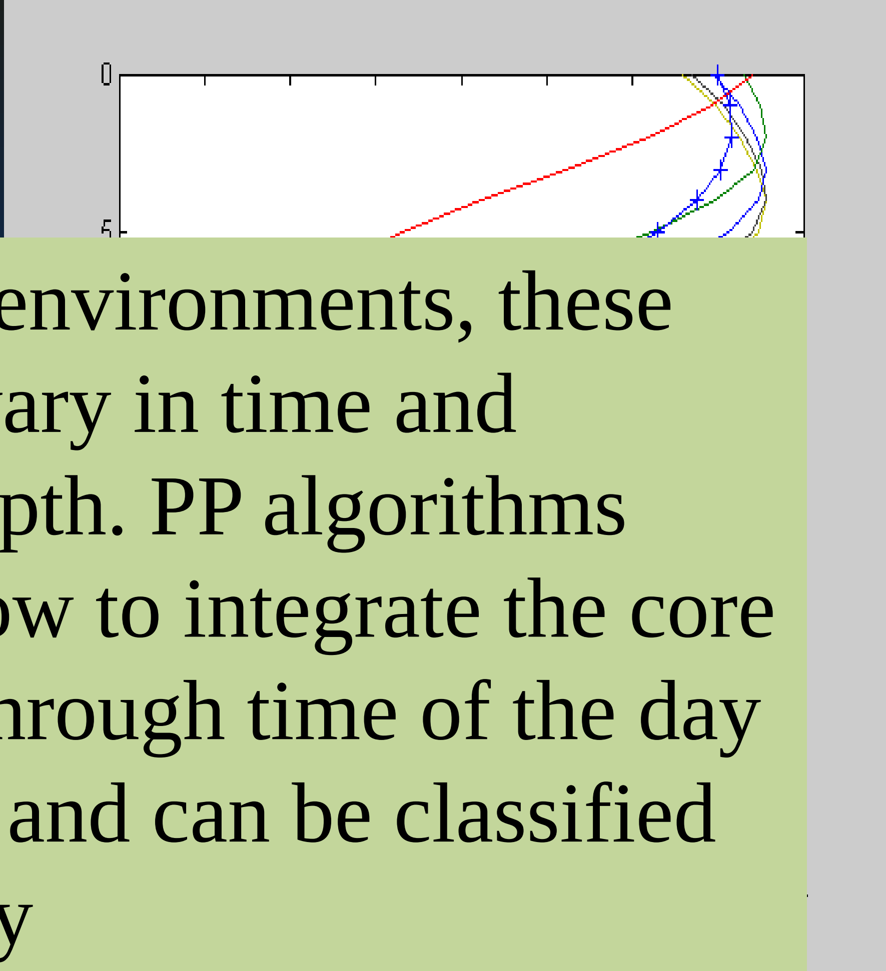

In aquatic environments, these variables vary in time and through depth. PP algorithms differ in how to integrate the core variables through time of the day and depth, and can be classified accordingly

$$\Sigma PP = \int_{\lambda=400}^{700} \int_{t=sunrise}^{sunset} \int_{z=0}^{Z_{eu}} p(\lambda, t, z)\, d\lambda\, dt\, dz$$

$$= \int_{\lambda=400}^{700} \int_{t=sunrise}^{sunset} \int_{z=0}^{Z_{eu}} \Phi(\lambda, z) \cdot PAR(\lambda, t, z) \cdot a^*(\lambda, z) \cdot Chl(z)\, d\lambda\, dt\, dz$$

PP algorithms

- Numerous PP algorithms have been compared against the in-situ observations (Campbell et al., 2002; Friedrichs et al, 2009; Saba et al, 2010; Saba et al., 2011).
- Regardless of the exact formulations, these algorithms have three core variables: phytoplankton biomass (or absorption), biomass-specific photosynthetic rate (or quantum yield of photosynthesis), and Z_eu.

3 core variables in PP estimation

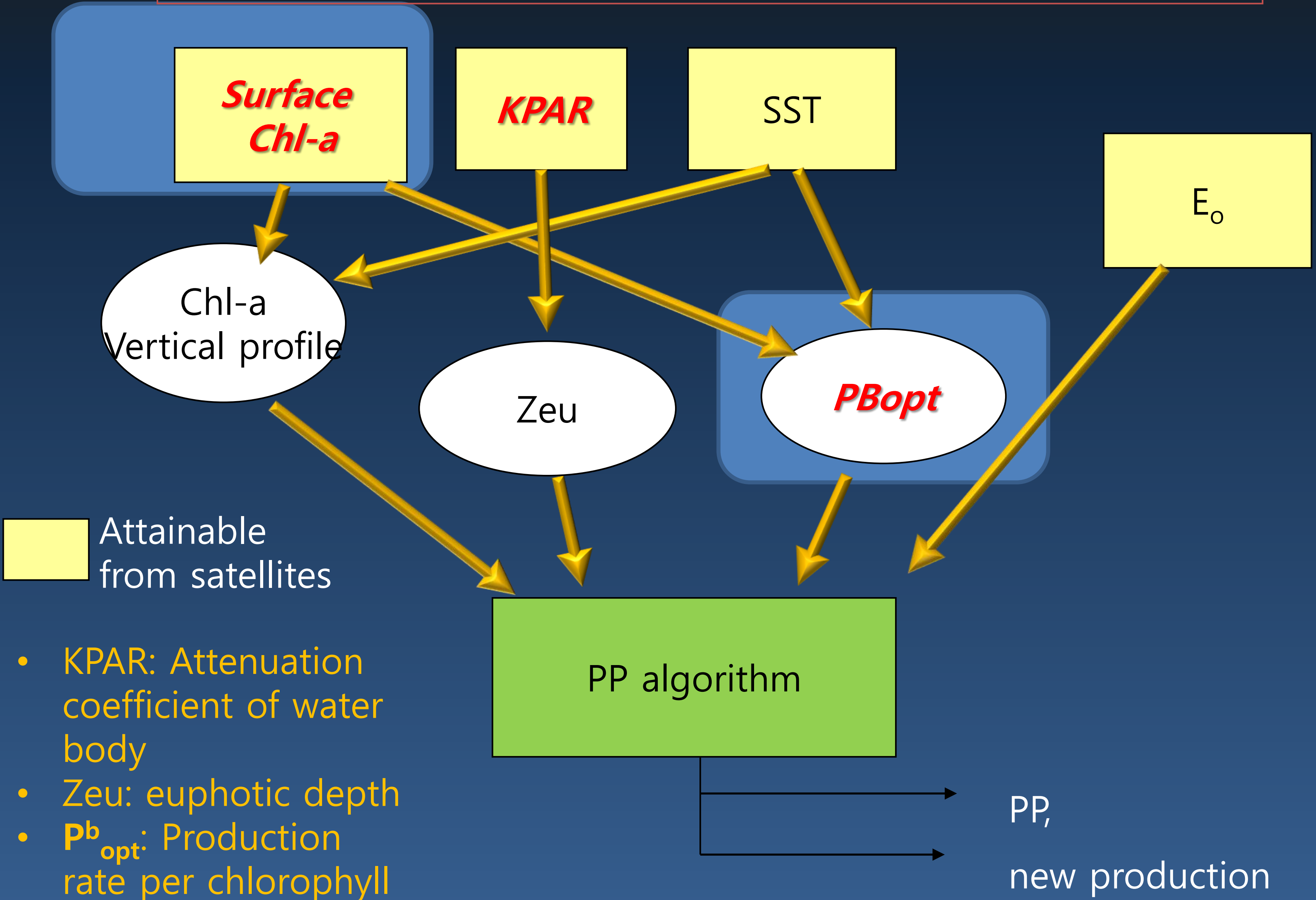

Surface Chl-a

KPAR

SST

E_o

Chl-a Vertical profile

Zeu

PBopt

🟨 Attainable from satellites

PP algorithm

PP,

new production

- KPAR: Attenuation coefficient of water body
- Zeu: euphotic depth
- **P^b_{opt}**: Production rate per chlorophyll

Core Var 1: Chl-a

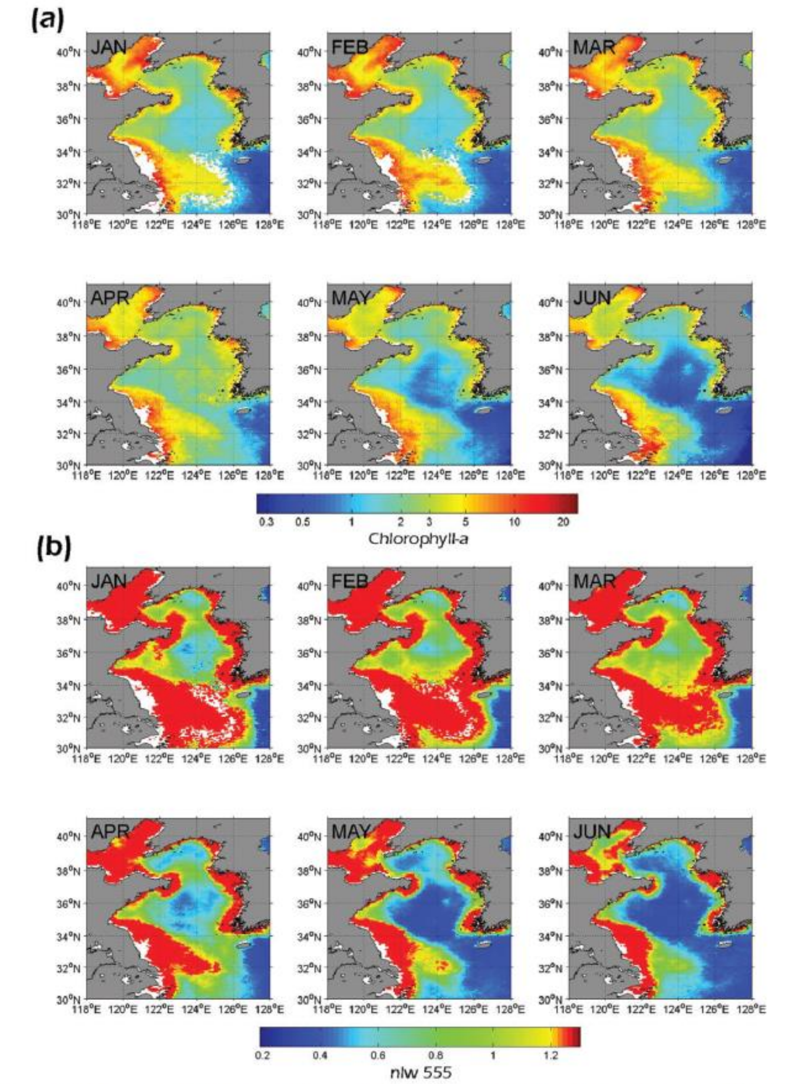

Fig. 2. Climatology (1998-2007) of (a) chlorophyll-a concentration (mg m^{-3}), and (b) normalized water leaving radiance (nW cm^{-2} μm^{-1} sr^{-1}) at 555 nm in the Yellow Sea from January to June. SeaWiFS OC4v4 standard algorithm was used for chlorophyll-a

Park and Yoo (2010)

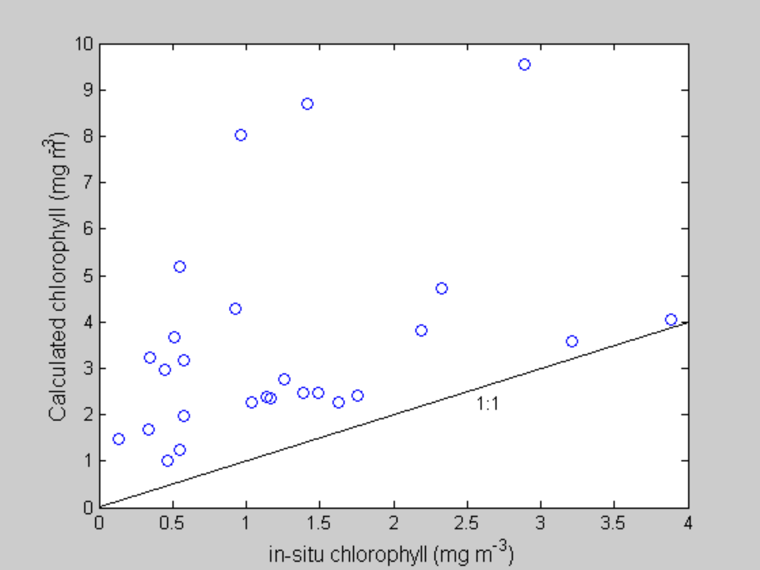

Comparison of CHL by OC4 (standard) algorithm and in-situ CHL

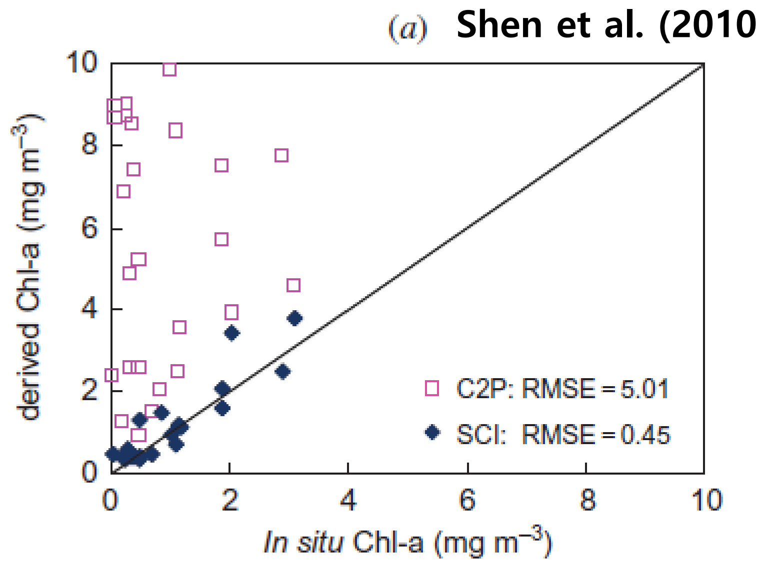

Shen et al. (2010)

Figure 7. *In situ* Chl-*a* versus derived Chl-*a*. Fi

Core Var 1: Chl-a

Yellow Sea Ocean Color Database

(Bio-optical measurements)

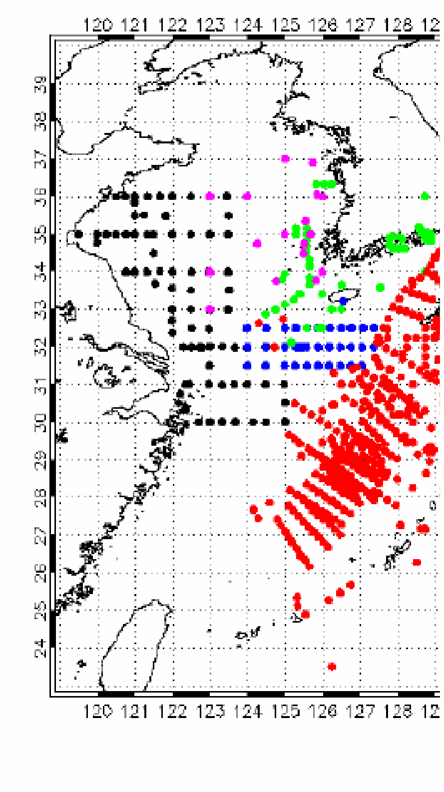

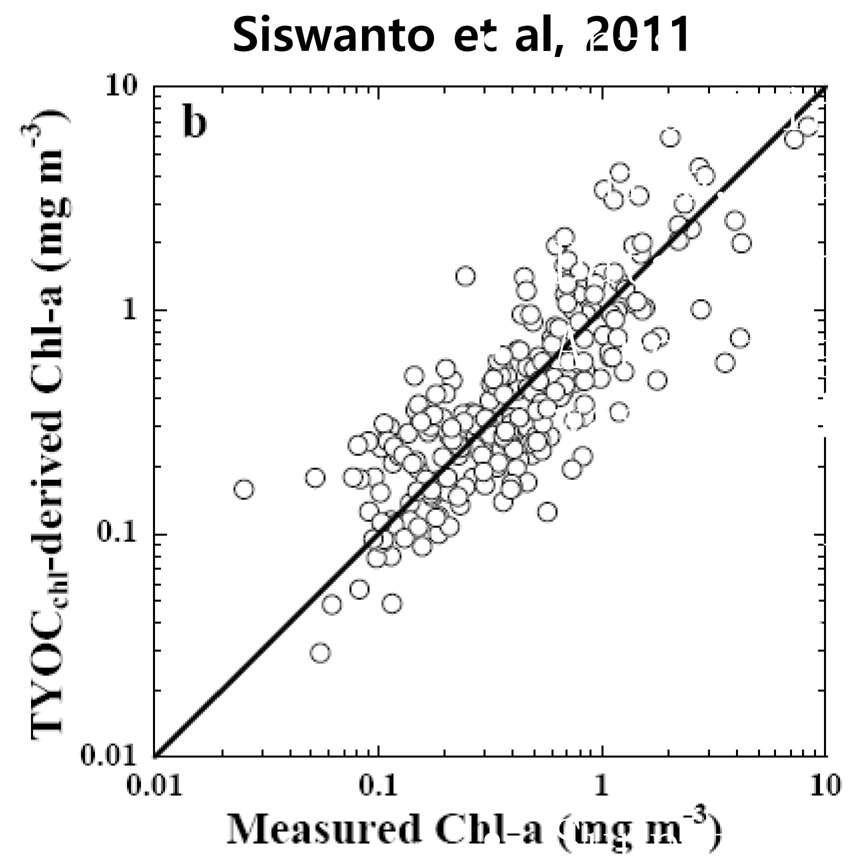
Siswanto et al, 2011

-optical data
itutions in
n and Korea
> 700
nal algorithm
d:
y tuned to the
ers in the Yellow
st China Sea
ctral bands

y YSLME
Project

Core Var 2: biomass-specific photosynthetic rate

Comparison of P_B^{opt} algorithms

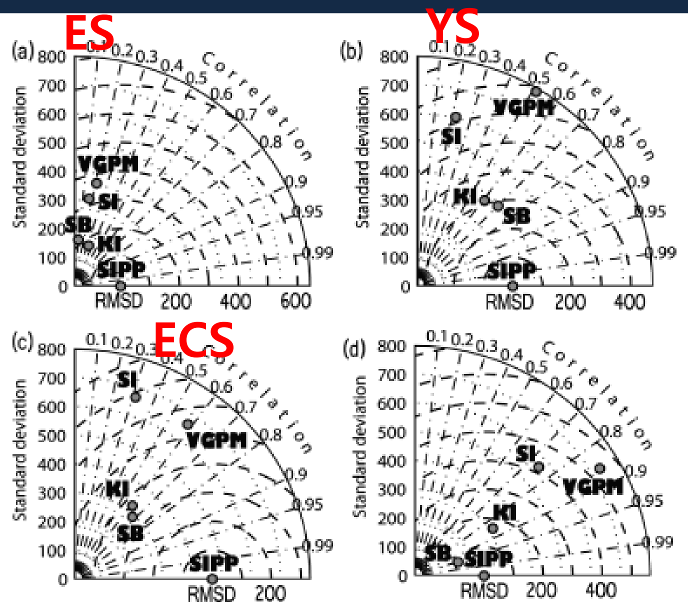

Fig. 9. Region-wise Taylor diagrams displaying STD, RMSD, and correlation for the four NPP algorithms in (a) ES, (b) YS, (c) ECS, and (d) YEOSU. The distance from the origin is the standard deviation of the modeled IPP (NPP). The azimuth angle represents the correlation between SIPP (NPP = GPP × 0.9) and modeled IPP (NPP), and distance between modeled IPP (NPP) and SIPP (NPP = GPP × 0.9) is the RMSD

Yoon et al. (2012)

$$\mathrm{IPP} = 0.66125 \times P^{B}_{opt} \times \frac{E_0}{E_0 + 4.1} \times Z_{eu} \times \mathrm{SCHL} \times D_{irr}$$

$$P^{B}_{opt} = -3.27 \times 10^{-8} \times \mathrm{SST}^7 + 3.4132 \times 10^{-6} \times \mathrm{SST}^6 - 1.348 \times 10^{-4} \times \mathrm{SST}^5 + 2.465 \times 10^{-3} \times \mathrm{SST}^4 - 0.0205 \times \mathrm{SST}^3 + 0.0617 \times \mathrm{SST}^2 + 0.2749 \times \mathrm{SST} + 1.2956$$

Behrenfeld and Falkowski (1997)

$$P^{B}_{opt} = \frac{0.071 \times \mathrm{SST} - 3.2 \times 10^{-3} \times \mathrm{SST}^2 + 3.0 \times 10^{-5} \times \mathrm{SST}^3}{\mathrm{SCHL}} + (1.0 + 0.17 \times \mathrm{SST} - 2.5 \times 10^{-3} \times \mathrm{SST}^2 - 8.0 \times 10^{-5} \times \mathrm{SST}^3)$$

Kameda and Ishizaka (2005)

Core Var 3: Z_{eu}

Table 1. The four major approaches to derive the Z_{eu} from satellite observation

Approach	Algorithm	Reference
(a) *Chl-a* based empirical model	$\boldsymbol{Zeu_{1\%}} = 34.0(Chl)^{-0.39}$	(Morel and Berthon, 1989)
	<u>*Calculation for the*</u> Z_{eu} *:* $\boldsymbol{Zeu_{1\%}} = \frac{4.605}{K_d(PAR)}$	
(b) Single empirical model	$\boldsymbol{K_d(PAR)} = 0.6677 \times K_d(490)^{0.6763}$ $\boldsymbol{K_d(PAR)} = 0.0864 + 0.884 \times K_d(490) - 0.00137 \times K_d(490)^{-1}$	(Pierson et al., 2009) (Morel et al., 2007)
(c) Switching empirical model	$\boldsymbol{K_d(PAR)} = (1 - \mathrm{W}) \times K_d{}^{Clear}(PAR) + W \times K_d{}^{Turbid}(PAR)$ Where, $K_d{}^{Clear}(PAR) = K_d(PAR)$ algorithm by M*orel et al.* (2007) $K_d{}^{Tubid}(PAR) = 0.8045 \times K_d{}^{turbid}(490)^{0.917}$ by Wang et al. (2009) $K_d{}^{turbid}(490) = -0.05256 + 1.3537\left(\frac{R_{rs}(670)}{R_{rs}(490)}\right)$ $\mathrm{W} = -1.175 + 4.512\left(\frac{R_{rs}(670)}{R_{rs}(490)}\right)$ for $[0.2604 \leq \frac{R_{rs}(670)}{R_{rs}(490)} \leq 0.4821]$ W=0 for $[\frac{R_{rs}(670)}{R_{rs}(490)} < 0.2604]$ W=1 for $[\frac{R_{rs}(670)}{R_{rs}(490)} > 4.821]$	(Son & Wang , 2015; Wang et al., 2009)
(d) IOP-centered semi-analytical model	1. a(490) and $b_b(490)$ were derived from R_{rs} using Quasi-Anlytical algorithm version 5 2. $K_d(PAR)(Z)$ was calculated using a(490), $b_b(490)$, and sun angle (θ_s) 3. Finally, $Zeu_{1\%}$ was calculated	(Lee et al., 2002, 2005 & 2007)

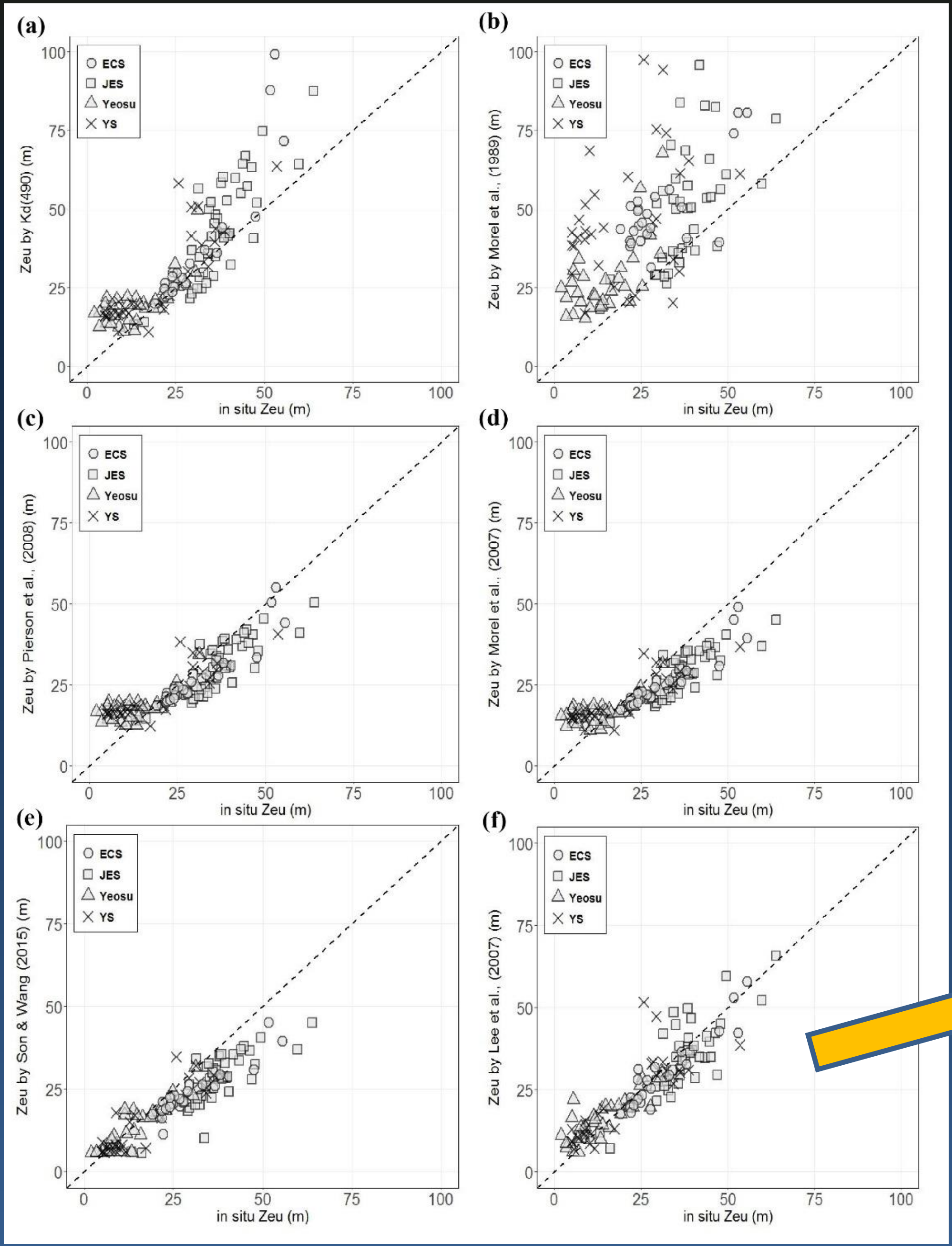

Performance of six K_d *(PAR)* algorithms using the in situ measurements made in the YS, ECS, and JES LMEs from 1994 to 2011 (n=32 (YS); n=55 (ECS); n=41 (JES)).

The IOP-centered algorithm showed lowest errors in terms of bias, RMSE, MAE, and absolute relative difference.

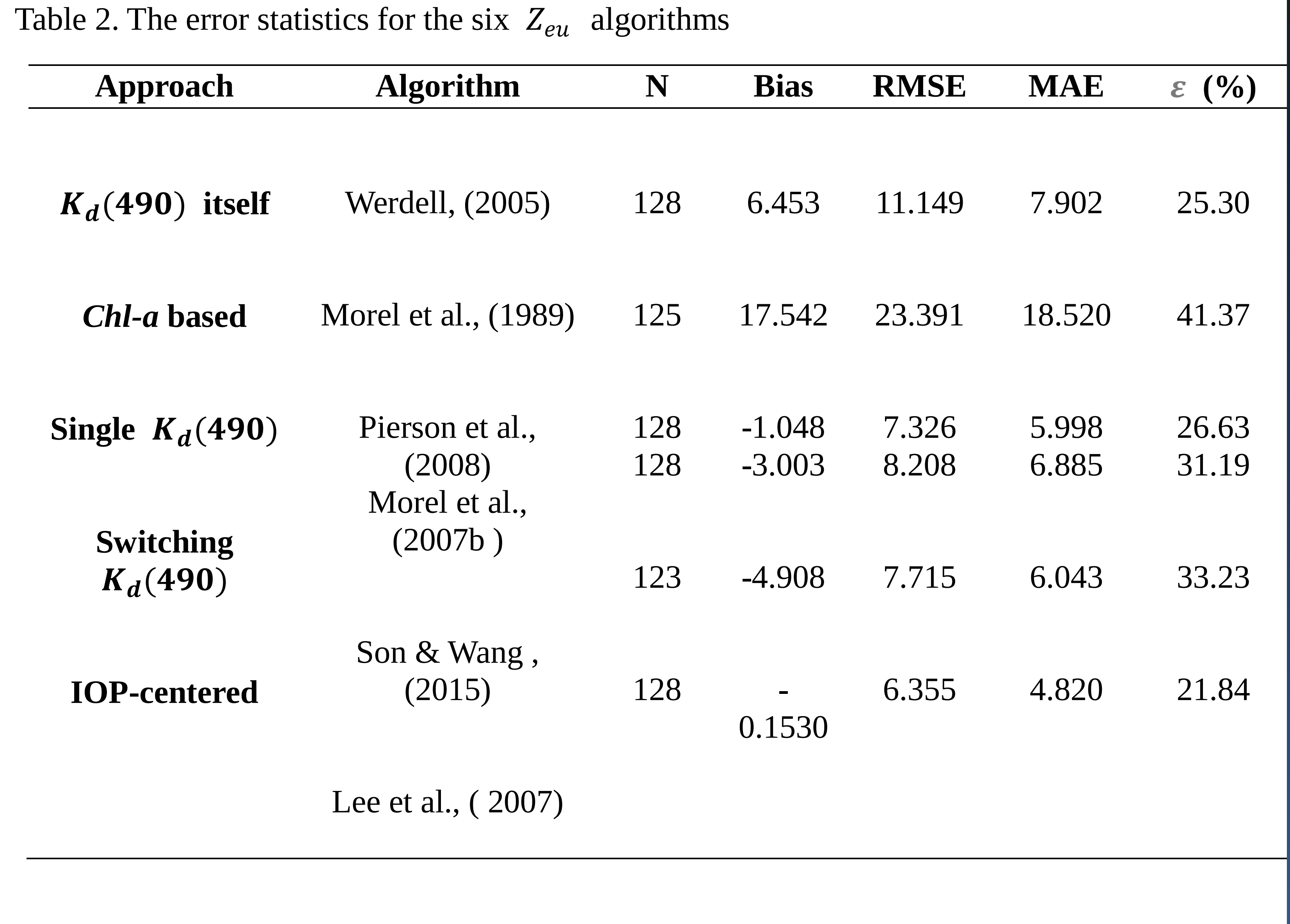

Table 2. The error statistics for the six Z_{eu} algorithms

Approach	Algorithm	N	Bias	RMSE	MAE	ε (%)
$K_d(490)$ itself	Werdell, (2005)	128	6.453	11.149	7.902	25.30
***Chl-a* based**	Morel et al., (1989)	125	17.542	23.391	18.520	41.37
Single $K_d(490)$	Pierson et al., (2008)	128	-1.048	7.326	5.998	26.63
		128	-3.003	8.208	6.885	31.19
	Morel et al., (2007b)					
Switching $K_d(490)$		123	-4.908	7.715	6.043	33.23
IOP-centered	Son & Wang , (2015)	128	-0.1530	6.355	4.820	21.84
	Lee et al., (2007)					

Data

- Satellite data

  SeaWiFS and MODIS/Aqua (1998~2014)
  - CHL-a:
    - OC4 v6 (NASA, 2010)
  - SST
  - PAR
- Algorothms
  - YOC for Chlorophyll-a (Siswanto et al., 2011)
  - Photosynthetic rates (Kameda and Ishizaka, 2005)
  - Euphotic depth (ZP Lee, 2005 and 2007)

The mean annual *PP* estimated by three methods (unit:$gC\ m^{-2}\ y^{-1}$)

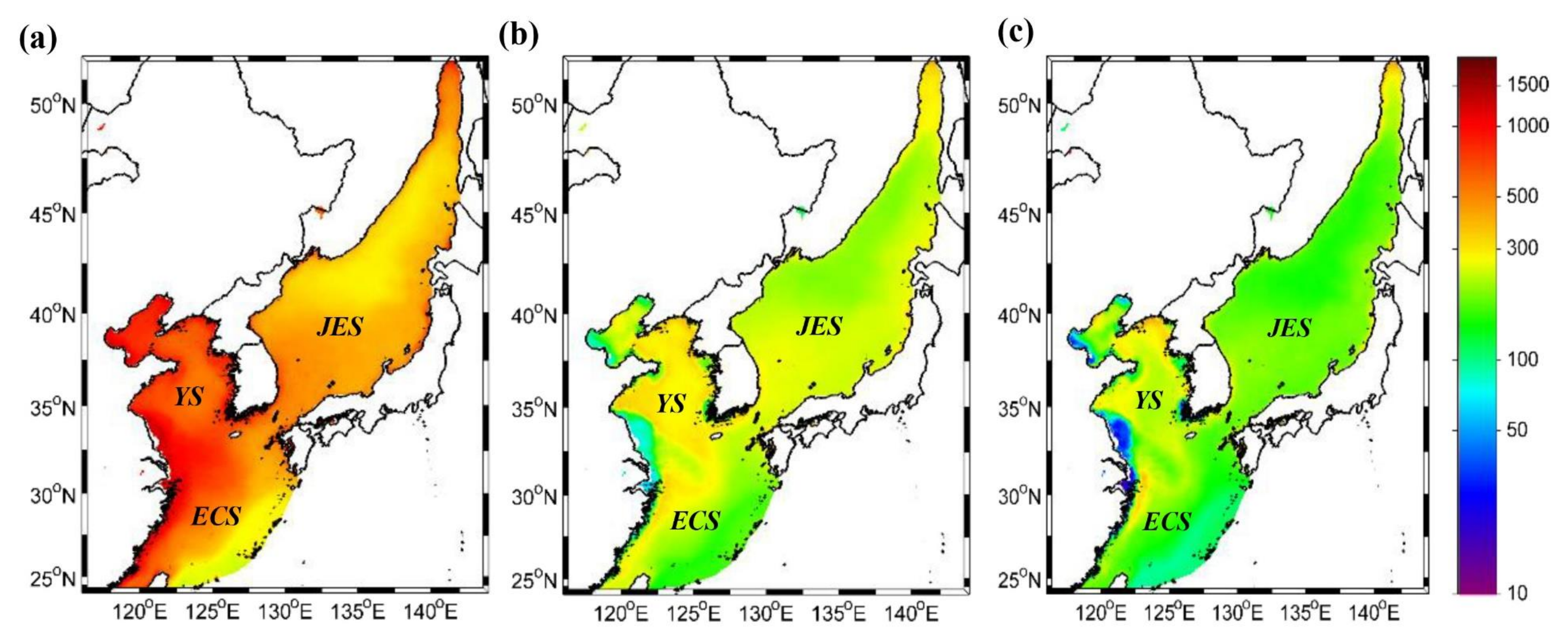

	Method-1	Method-2	Method-R
Chl-a	NASA	YOC	YOC
P_B^{opt}	B-F	K-I	K-I
Z_{eu}	$K_d(490)$	$K_d(490)$	IOP-centered

Table 3. The mean annual *PP* estimates by the three methods *(gC m-2 y-1).* The numbers in the parenthesis indicate the range in 1998-2014 period.

	YS	ECS	JES
Method - 1	778 (770~857)	545 (485~590)	420 (362~466)
Method – 2	259 (248~272)	222 (213~229)	248 (215~255)
Method - R	211 (189~247)	165 (156~170)	193 (178~204)

Primary Productivity

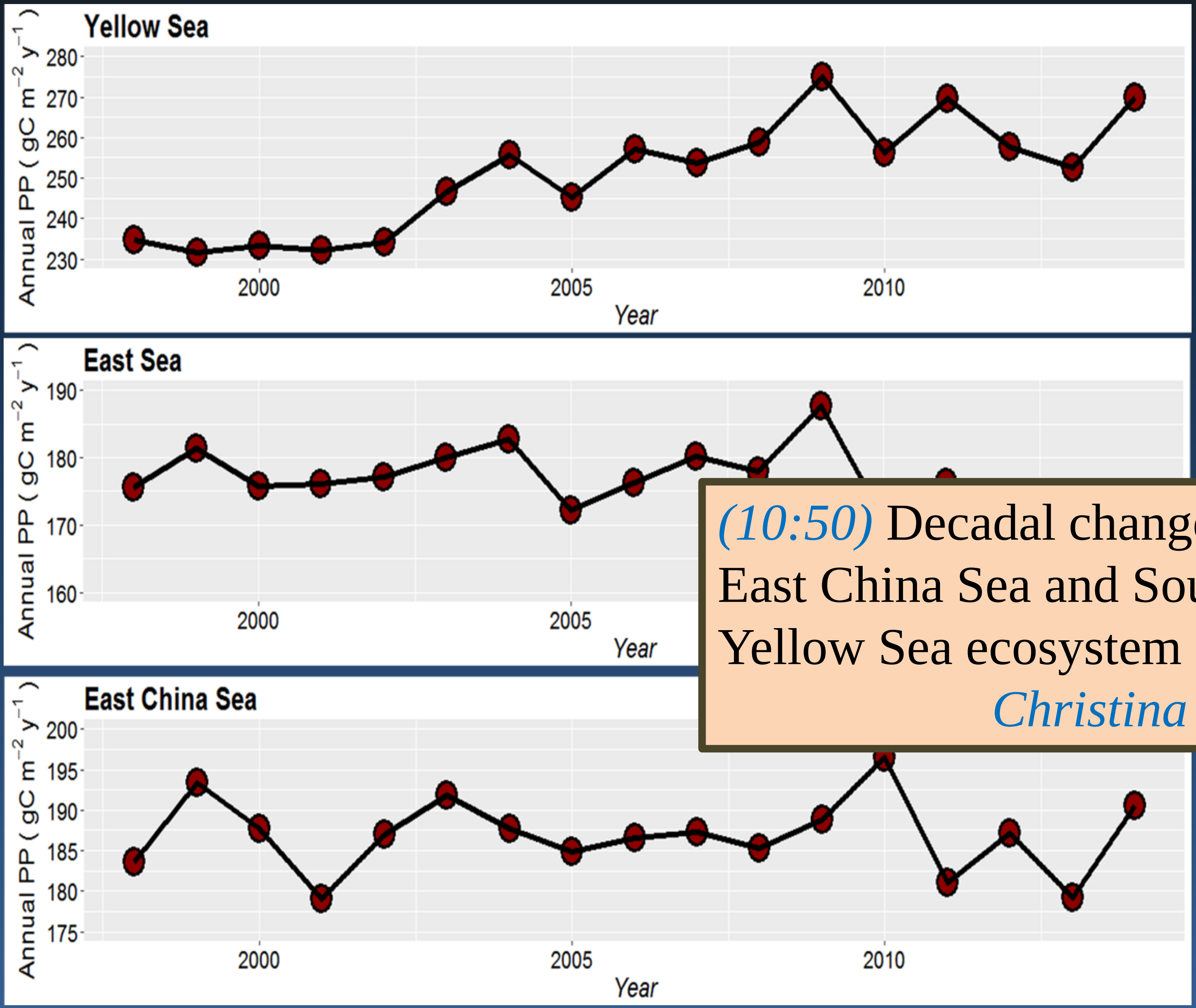

(10:50) Decadal changes in the East China Sea and Southern Yellow Sea ecosystem | *Christina Eunjin Kong*

PP models of other global assessments

- LME/UNEP Report (2008): Ocean Productivity from Absorption and Light (OPAL) model (Marra et al., 2003) → an absorption-based model

- Sea around Us Project: Platt and Sathyendranath (1988) with parametrization based on biogeochemical provinces. → a time and depth-resolved model.

Comparison of the mean annual PP by three methods of this study, the SAU Project, and the UNEP/LME Report.

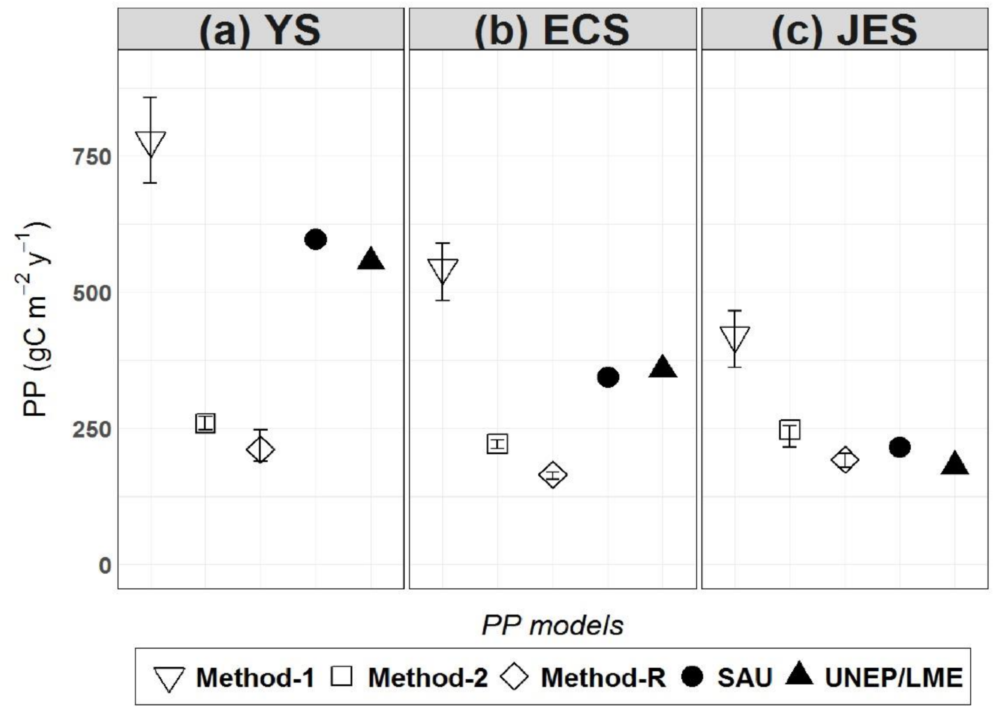

Revised with new PP estimates

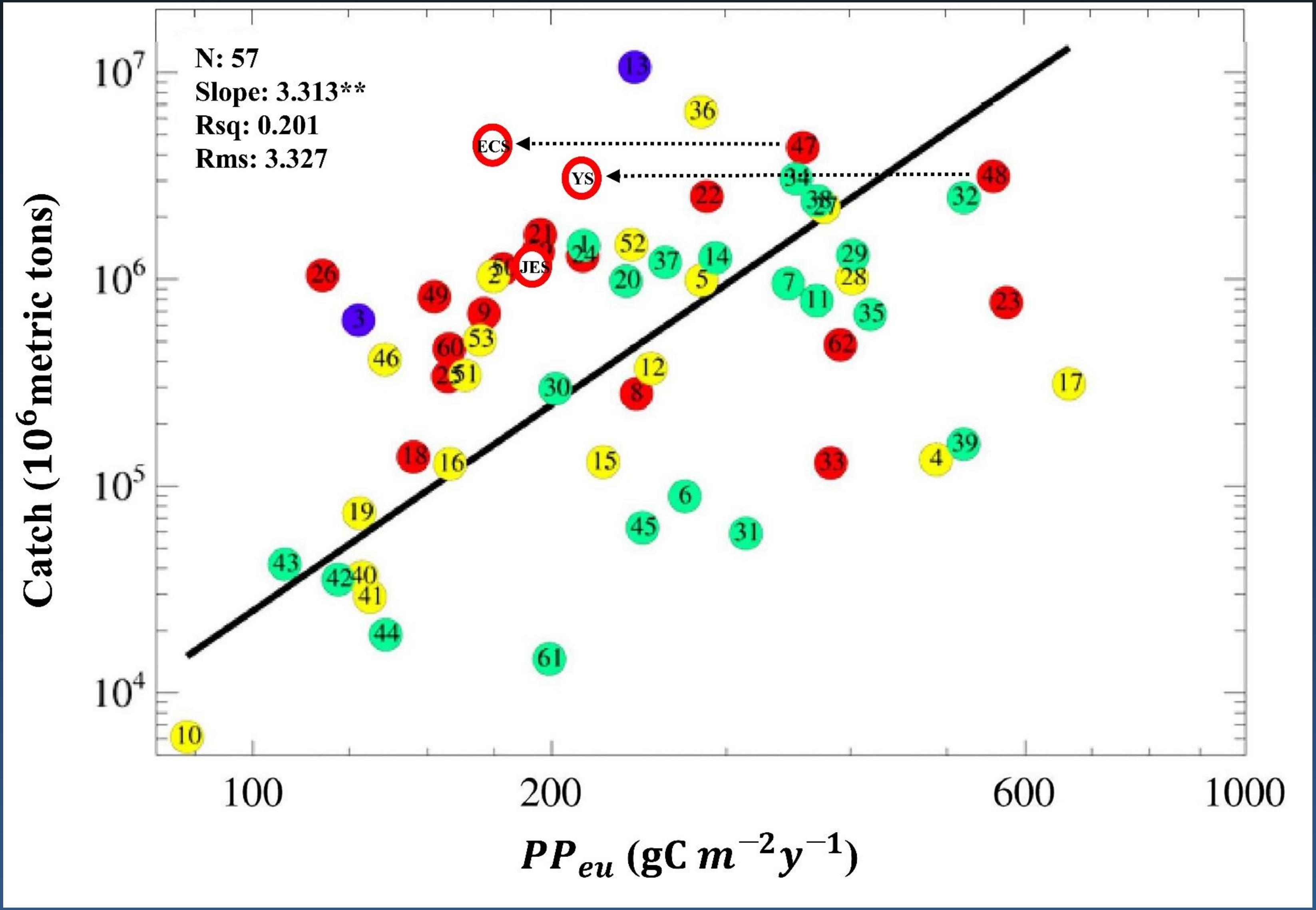

UEP LME Report,
Sherman and Hempel (2009)

Conclusions

1) Accurate parametrization of the core variables is more important than choosing a primary productivity model, and
2) The previous global LME assessments might have overestimated the annual primary productivity in the Yellow Sea by a factor of 2 or so.

Thank you!

Classification system for daily net primary productivity (NPP) models based on implicit levels of integration

(Behrenfeld and Falkowski, 1997)

I. Wavelength-resolved models (i.e., "bio-optical models")(WRMs)

$$NPP = \int_{\lambda=400}^{700} \int_{t=sunrise}^{sunset} \int_{z=0}^{Z_{eu}} \Phi(\lambda, Z) \cdot PAR(\lambda, t, z) \cdot a^*(\lambda, z) \cdot Chl(z) d\lambda dt dz - R$$

II. Wavelength-integrated models (WIMs)

$$NPP = \int_{t=sunrise}^{sunset} \int_{z=0}^{Z_{eu}} \varphi(z) \cdot PAR(t, z) \cdot Chl(z) dt dz - R$$

III. Time-integrated models (TIMs)

$$NPP = \int_{z=0}^{Z_{eu}} P^B(z) \cdot PAR(z) \cdot DL \cdot Chl(z) dz$$

IV. Depth-integrated models (DIMs)

$$NPP = P_{opt}^B \cdot PAR(0) \cdot DL \cdot Chl \cdot Z_{eu}$$

PP estimates from the previous studies

- Point measurements vary in the range of 11.78 ~ 3,175 mg C m^{-2} d^{-1} depending on time and space.
- Some of in-situ estimates on annual production are 135˜265 gC m^{-2} y^{-1}, which is much smaller than satellite estimates.
- Park and Yoo (2010) compared 4 chlorophyll X 2 PP algorithm combinations: 96.5 to 610.2 gC m^{-2} yr^{-1}.
- Tan and Shi (2006) using SeaWiFS-MODIS 2003-2005 and VGPM formulation,
  - Bohai Sea: 564.4 gC m^{-2} y^{-1}
  - Northern Yellow Sea: 363.1 gC m^{-2} y^{-1}
  - southern YS: 536.5 gC m^{-2} y^{-1}
  - northern East China Sea (ECS): 413.9 gC m^{-2} y^{-1}
  - southern ECS: 195.8 gC m^{-2} y^{-1}